APPLIED GEOPHYSICS, Vol.18, No.3 (September 2021), P. 420–430, 15 Figures.
DOI:10.1007/s11770-021-0907-1

Integrating the geology, seismic attributes, and production of reservoirs to adjust interwell areas: A case from the Mangyshlak Basin of West Kazakhstan*

Arslan Zhumabekov♦[1,3], Zhen Liu[1], Vasily Portnov[2], Xiaodong Wei[3], and Xin Chen[3]

Abstract: Dynamic models of the seismic, geological, and flow characteristics of a reservoir are the main tool used to evaluate the potential of drilling new infill wells. Static geological models are mainly based on borehole data combined with dynamic analyses of production dynamics. They are used to determine the redevelopment of and adjustments to new drilling locations; however, such models rarely incorporate seismic data. Consequently, it is difficult to control the changes in geological models between wells, which results in the configuration of well positions and predicted results being less than ideal. To improve the development of adjusted areas in terms of their remaining oil contents, we developed a new integrated analysis that combines static sediment modelling, including microfacies analysis (among other reservoir and seismic properties), with production behaviours. Here, we illustrate this new process by (1) establishing favourable areas for static geological analysis; (2) studying well recompletion potential and the condition of non-producing wells; (3) conducting interwell analyses with seismic and sedimentary data; (4) identifying potential sites constrained by seismic and geological studies, as well as initial oilfield production; (5) providing suggestions in a new well development plan.
Keywords: Reservoir geological model, sedimentary facies, seismic attributes, well development, remaining oil

Introduction

Here, we present a case study of an oil field in the Mangyshlak Basin of West Kazakhstan, which has many operational reservoir intervals. Previous studies in the South Mangyshlak Sub-basin have indicated that the Middle Jurassic reservoir interval may be subdivided into thirteen productive units. Fine-to medium-grained fluvial (channel) sandstones with typical permeabilities of 6–115 mD (maximum: 239 mD) constitute the main reservoir facies; reservoir quality is severely impaired by

Manuscript received by the Editor January 12, 2021; revised manuscript received April 27, 2021.
1. State Key Laboratory of Petroleum Resource and Prospecting in China University of Petroleum, Beijing 102249, China.
2. Karaganda State Technical University, Karaganda, 100027, Kazakhstan.
3. BGP Inc., China National Petroleum Company CNPC, Zhuozhou 072751, China
♦Corresponding author: Arslan Zhumabekov (E-mail: zhak28@gmail.com).

the amount of clay and carbonate cement, which may reach 50% of the bulk rock volume regionally (Ulmishek, 2001). The reservoir is strongly layered, with numerous lacustrine to shallow marine shale layers occurring both between and within the productive units, effectively partitioning the stratigraphic section and giving rise to multiple hydrocarbon–water contacts. Reservoir units are internally heterogeneous with only moderate vertical connectivity and unidirectional lateral connectivity dictated by channel orientation. An interpretation of a newly acquired three-dimensional (3-D) seismic survey in the northwest of the field was scheduled to guide new drilling activities, beginning in early 2008; however, data on the drilling status are currently unavailable.

To further petroleum exploration in this basin, it is necessary to re-evaluate its constituent reservoirs. Reservoir redevelopment planning combined with seismic correlations can be used to predict the remaining volume and distribution of hydrocarbons, thereby promoting petroleum exploration (Gunter *et al.,* 1997; Carter, 2003; Tang *et al.,* 2019). However, no studies involving the seismic correlation of the reservoirs in the Mangyshlak Basin have been conducted. In this study, seismic and geological facies, along with the dynamic operating conditions, were considered for the development interval of the target horizon (J-III) to establish the remaining oil potential. We first evaluated the primary favourable zones, so that our analyses of seismic attributes were conducted in areas with high effective thicknesses, favourable sedimentation, and large potential remaining oil volumes. Secondly, the dynamic properties were defined, the study of which focused mainly on the following parameters: oil and water migration in areas with little restriction by the well grids, areas with limited depletion, and areas with low water cuts after development. Here, we promote the further opportunities for find remaining oil through drilling new wells and re-invigorating idle wells (Arslan *et al.,* 2019).

Geological setting and static analysis

The Mangyshlak Basin is located on the eastern coast of the Middle Caspian Sea, primarily in West Kazakhstan (Figure 1). The basin continues into Uzbekistan and Turkmenistan in the east and south, respectively. The structural terrace on the northern margin of the South Mangyshlak Sub-basin in the Middle Caspian Basin (Kiritchkova *et al.,* 1983) hosts the majority of the oil and gas fields (Soloviev *et al.,* 2017). The Middle Caspian Basin (Kazhegeldin, 1997; Effimov et al., 2001; Lechner *et al.,* 2016) is floored by continental terrane that accreted onto the southern margin of the Eurasian Plate during the Permian. Its sedimentary fill consists of up to 12 km of predominantly Mesozoic strata (Aliyeva, 2009) in a large inverted rift.

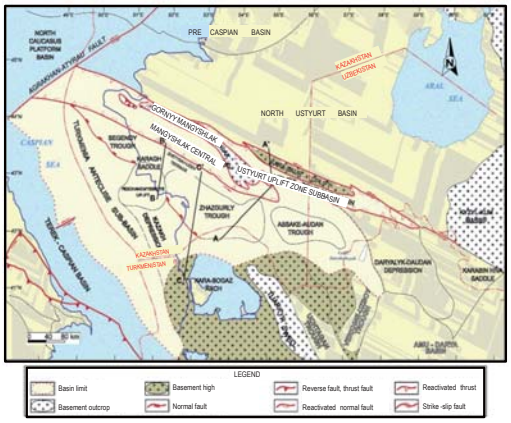

Figure 1. Location of the Mangyshlak Basin.

The structural development of the Mangyshlak Sub-basin began during the Late Permian–Triassic, when rifting created a large west–northwest (W–NW) graben over the Mangyshlak uplift zone. It was initially filled with a thick interval of clastic continental sediments, transitioning to a marine sedimentary basin with local volcanic horizons in the Middle–Late Triassic. The uppermost Lower Triassic–Middle Triassic shales are the likely source of most of the hydrocarbons in in South Mangyshlak fields (Ulmishek, 1990, 2001).

To visualise different sedimentary environments and their representative facies (Zudakina *et al.,* 1980), core and logging data, petrophysical parameters (Gunter *et al.,* 1997; Pennington, 1997; Zhang *et al.,* 2016), reservoir summaries (Berkhout, 1993; Walls *et al.,* 2004), and sedimentary facies types are needed; the separations among the facies in individual wells are marked on seismic profiles (Posamentier, 2000; Harilal *et al.,* 2008; Avseth *et al.,* 2010; El-Mowafy *et al.,* 2016) and geological maps (Jing *et al.,* 2014; Tang *et al.,* 2019). To improve the continuity of sand bodies, we combine microfacies characteristics and seismic data with the root mean square (RMS) seismic attribute (Brown, 1996; Chopra *et al.,* 2005, 2014). Furthermore, to identify the main productive

zones and potential areas with remaining oil, the initial oil production rates, water cuts, and cumulative productions of well were correlated with the current information.

Reservoir architecture

Oil and gas accumulations occur in very heterogeneous reservoirs due to their deposition in fluvial channels and associated facies. Each of the thirteen productive Middle Jurassic reservoir units of the South Mangyshlak Sub-basin typically comprise two to eight discontinuous sandstone layers. The oil pay in individual reservoir units is 1.3–21.2 m and gas pay is 2–14.4 m (Kazhegeldin, 1997). Continuous mudstone layers, typically 1–20-m-thick, separate the reservoir units, which act as separate flow layers. Vertical connectivity within reservoir units ranges from moderate to poor, owing to the moderate abundance of mudstone layers. Lateral connectivity is higher because of the braided channel belts (200–700-m-wide in the nearby Uzen Field) but are unidirectional and in line with the dominant SW-trending channel orientation.

Sedimentary facies

Analysing seismic and log phases allows us to predict the distribution of sedimentary microfacies (Muruthy *et al.,* 2018) *per* reservoir interval in a study area (Figure 2). Horizons J-I to J-XI were interpreted as delta front deposits, with interbedded sands and mud, an overall fine grain size and multi-stage upward-coarsening reverse sequence. The submarine distributary channel is the main reservoir facies, with the mouth bar and distal bar serving as secondary reservoirs. Horizons J-XII to XIII were interpreted as braided channels with thick, clean sand layers, coarse particle sizes, and a stable depositional history; they are the main reservoir rocks in these horizons.

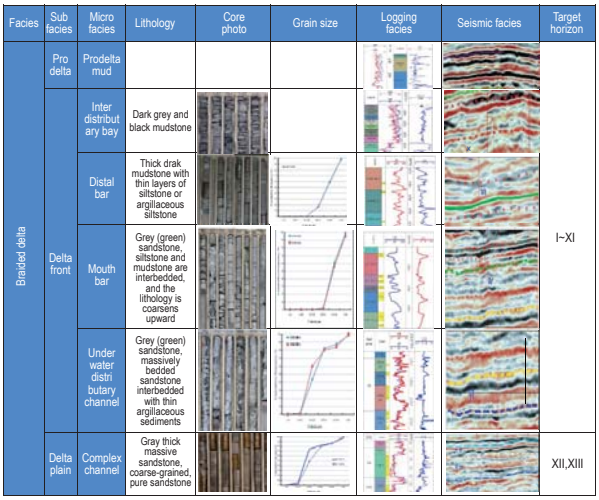

Figure 2. Lithology, grain size, logging data, and seismic profiles of sedimentary (micro) facies.

Depositional heterogeneity greatly impacts the distribution and areal extent of sedimentary microfacies. From the map of facies in horizon J-III (Figure 3), it is evident that the sediment was sourced from the north, with four 4-branched deltas, and the channel sand bodies spread in a wide strip in the near N–S strike direction. The width of the four zones of channel development in the north ranges from 3 to 7 km and these represent the main reservoirs. In the south, the sand bodies of distal estuarine sand bars are developed and serve as secondary reservoirs.

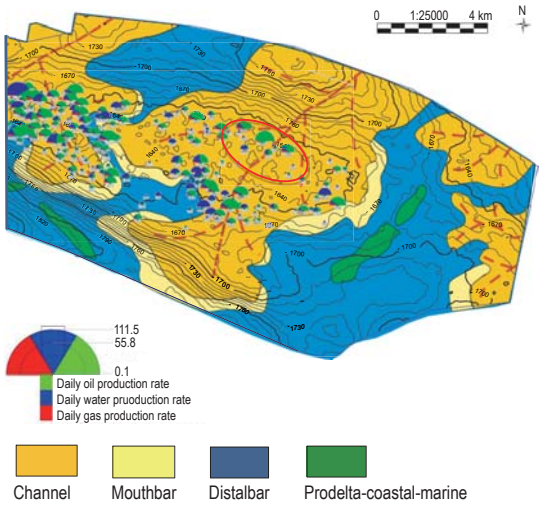

Figure 3. Overlay map of the initial productivity, sedimentary microfacies, and structure of horizon J-III.

Reservoir properties and relationships

The relationship of the lithology, physical property, electrical property, oiliness and between each other is called the four-property relationship of the reservoir (Li et al., 2011). The four-property relationship of the reservoir is an important basis for the interpretation of the oil-water layer and the evaluation of reservoir (Chen et al., 2010). In general, the reservoir rock have more better physical properties of the coarse particles, but the physical property of reservoir is obviously influenced by the type and content of cement. The higher content of cement, the lower porosity and permeability, and the influence of cement content on permeability is greater than the effect on the porosity. The content of carbonate rock has a strong influence on the permeability, but the

influence on the porosity is not obvious. In addition, the chink has a certain impact on the property, with the increase of the filler content; the reservoir performance has a trend to go bad. The reliability of various understandings and petrophysical relationships depends on the consistency between the rock characteristics of existing core materials and those of the rocks covered with pay zones. In order to evaluate the physical properties of Jurassic reservoir rocks in oilfield, the results of all representative core samples analyzed are used. When calculating the average value of reservoir parameters of each layer, the reservoir is not divided according to saturation. The research results of lithologic lithofacies and electrical characteristics of rocks are the petrophysical basis for interpretation of geophysical logging data.

Correlation between porosity and permeability of rocks. Comparing the porosity permeability relationship obtained according to the core research results shows that there is no significant difference in the correlation relationship among the rocks of different pay zones studied. The relationship between porosity and permeability has a very low correlation coefficient for each layer formation. Because the unified boundary values of all strata have been completely determined earlier, different correlation relations have been obtained. In order to solve this problem, unify the J-I - J-IX layer and J-XII – J-XIII layer, and calculate the average porosity according to the permeability grade (0.01 - 0.02; 0.02-0.05; 0.05-0.1, etc.). The obtained correlation between permeability and porosity shows that there is a comparison relationship between these parameters, and the comparison coefficient is very high. The porosity limit of J-I - J-XI and J-XII – J-XIII is 12.6 and 8.8 respectively when the permeability is 7mD, which confirms the porosity value previously used.

Rock density and grain porosity. For the relationship between grain porosity and density of Jurassic strata, there is no differential, so there is a large deviation, and the correlation coefficient is not high. The equation describing the relationship is between values of porosity as function of density index.

The water saturation and oil saturation of rocks are determined by direct and indirect methods. The capillary pressure curve was drawn, and the average pore radius of samples collected from the production layer of oil field was calculated by lab method. This method is also used to deal with the results of the core capillary pressure curve. The results of water saturation measurement (direct method) of cores collected from wells are as mentioned above. The values are very low. As a result, the oil saturation increases. The results of determining water saturation and oil saturation of core samples by indirect method are used to evaluate the residual water saturation. The effective porosity of these core samples is determined to be 8% to 32%. The capillary pressure curve was drawn by centrifugation of 6 cycles. The capillary pressure achieved is 5.4 MPa. For the samples of J-1 - J-XI layers, the porosity changes from 0.151 to 0.322, and the permeability changes from 4.7 to 415 mD. For J-XII - J-XIII layers, the porosity changes from 0.164 to 0.338, and the permeability changes from 28.5 to 1437 mD. The remaining water saturation of layer J-1 - J-XI (at 3 MPa) is 0.73, and that of layer J-XII - J-XIII is 0.46.

Electrical characteristics of rocks. Rock resistivity of 57 samples was studied before reserve calculation. Resistance of rock. According to the resistance research results of columnar extracted cemented samples (formation water model with salinity of 150g/L), the relationship between electrical resistance parameter and porosity was determined.

To sum up all petrophysical studies, the reservoirs of the studied oilfield consist of poorly- to moderately-sorted, fine- to medium-grained arkoses and sublitharenites cemented by clays and carbonates. Regionally, clay content may reach up to 50% of the bulk rock volume (Ulmishek, 2001). Mean permeabilities are low (6–115 mD, maximum: 239 mD) and decline drastically with increasing clay content. Thick, coarser-grained channel sandstones are characterised by lower clay contents and therefore higher permeabilities. Median porosities range from 16–22% (Kazhegeldin, 1997). A dual-porosity system exists due to the secondary intergranular pores resulting from the dissolution of cements, and intragranular microporosity is formed by the partial leaching of feldspars (Smale et al., 1997). The distribution of larger, intergranular pores controls the overall permeability, which consequently shows no relationship with total porosity (Zudakina et al., 1980). Initial water saturations are relatively high (30–45% for oil and 38–44% for gas), likely due to the retention of water via micropores.

The results of core analyses in the study area revealed that the medium porosity in Jurassic deposits at the oilfield ranges from 14.7–19.8%. In this study, the

Median porosity was determined for the oil-bearing strata, and the highest percentage was found in the J-III horizon (19.8%). Meanwhile, the porosity of the J-XI oil horizon was relatively low (14.7%). The permeability of the 13 oil-bearing formations in the Jurassic sediments was highly variable, averaging between 42 and 116 mD. The mean permeability along the J-V production horizon had the highest value (119 mD); that of the J-XIII horizon was also quite high, at 117 mD. Compared with the aforementioned horizons, the mean permeabilities of horizons J-X and J-XI were relatively low, 43 mD and 44 mD, respectively. Thus, the 13 oil-bearing units are terrigenous reservoirs (sandstones) with medium porosity and medium permeability. The reservoirs within the productive horizons, J-XII to J-XIII, are represented by sandy coarse-grained sediments, and their median porosity may be underestimated relative to the overlying productive horizons, though the mean permeability is higher.

Application of seismic attributes

The seismic attribute in area also reflects well the characteristic of lithological variability. According to the Vp / Vs attribute, it was noted in the formation by area that in the central and eastern parts there is a high attribute anomaly expressed by "red" tones, respectively, "blue" tones are present between the eastern and central parts, which is, in its turn, a zone of lithological variability. This significantly coincides with the drilling data (Figure 4), therefore, using the Vp / Vs attributes in terms of area, it is possible to describe the zone of lithological variability, which provides the prerequisites for the analysis of water oil contact.

In the process of selecting individual wells with seismic attributes and inversion results, we mapped the sedimentary facies of these objects. Seismic attributes were selected and sensitivity analyses were performed. Different types of surface attributes (i.e. amplitude, frequency, phase, wave type) and drilling data were analysed and compared. The RMS attribute is suitable for countering the anomalous zones in the study area (marked in red in Figure 5). The seismic attributes were then analysed, including the reservoir RMS reflectivity and data on the well operation dynamics, and sedimentary microfacies characteristics were studied by area. Wells with high initial productivities were primarily located in the main reservoir — a branched channel with strong amplitudes (displayed in yellow in Figure 5). The sand body in the main channel is well developed and characterised by favourable petrophysical properties and low heterogeneity (Cao et al., 2005). Wells with low initial productivities were predominantly distributed beyond the edges of the channels (shown in green and blue in Figure 5). These areas contain thin sand bodies with poor connectivity and strong heterogeneity.

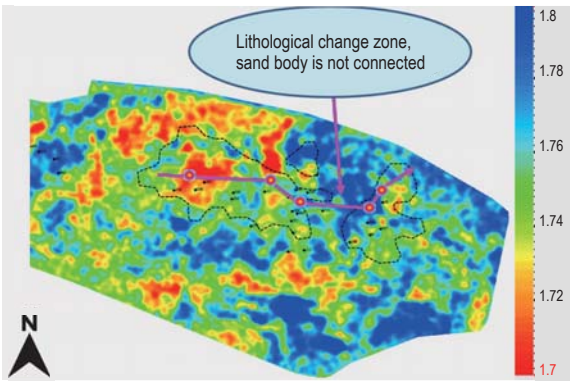

Figure 4. Vp / Vs attribute map by area along the productive horizon.

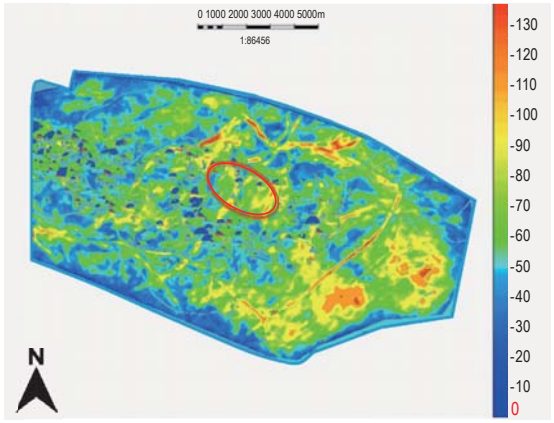

Figure 5. Overlay map of the initial productivity and RMS attribute of horizon J-III.

Experimental work-flow and methodology

Well recompletion potential

As a shallow horizon, J-III has been drilled in nearly every well throughout the region, and the operating well stock consists of 100 production and 42 injection wells across all reservoir layers. If J-III is to be redeveloped, the current dedicated well stock is insufficient and more wells will be needed. The recompletion of old wells originally drilled to develop deeper intervals should

allow us to economically and quickly resolve this problem. In horizon J-III, there are 24 recompleted wells from the underlying horizon (Table 1), of which nine are in the west and 15 are in the east; the maximum daily production rate of a single well is 188.26 bbl/d.

Table 1. Start time and initial oil production rate of the J-III horizon from recompleted wells from the underlying horizon.

Well	Start time of utilisation	Initial production rate J-III (bbl/day)
A	January, 2017	3.96
B	September, 2017	1.89
C	July, 2017	1.64
D	July, 2017	1.51
E	September, 2017	1.26
F	August, 2017	0.63
G	April, 2017	4.78
H	December, 2017	1.26
I	July, 2017	17.67
J	June, 2017	25.98
K	December, 2017	78.56
L	July, 2017	33.15
M	May, 2017	23.71
N	April, 2017	59.63
O	April, 2017	32.71
P	April, 2017	57.62
Q	October, 2017	67.68
R	May, 2017	81.14
S	February, 2017	57.05
T	August, 2017	54.53
U	August, 2017	188.26
V	November, 2017	35.92
W	July, 2017	12.89
X	July, 2017	22.58

From the overlay map of recompleted wells and RMS seismic attributes (Figure 6), high-production wells were found to correlate with stronger amplitudes, which indicates that seismic attributes can be used to predict

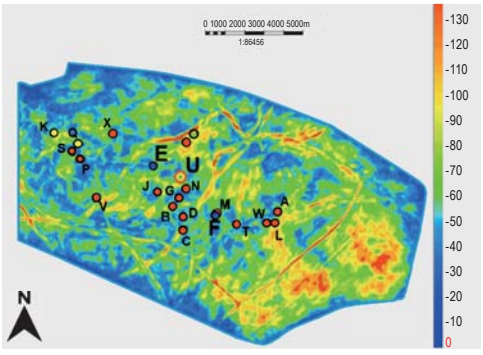

Figure 6. Overlay map of the initial productivity of recompleted wells from the underlying horizon and RMS attributes of J-III. Well labels correspond to those shown in Table 1.

reservoir properties. The cumulative oil production from recompleted wells from the underlying horizon of J-III reached 1.11 kbbl, with a daily oil production rate 369.06 bbl/d — equalling 8% of the total production of this horizon (Figure 7). Recompleting wells from the underlying horizon has therefore had a positive effect.

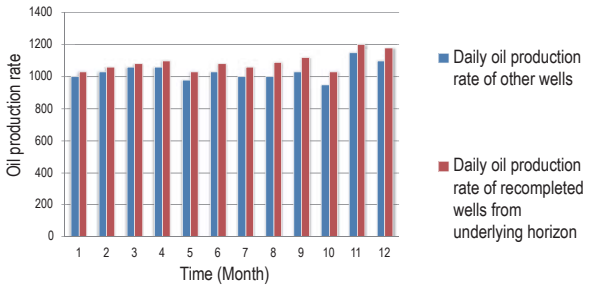

Figure 7. Production contributions of recompleted wells from the underlying horizon and other wells of J-III.

Currently, the percentage of idle wells in the study area is high, and the utilisation rate of old wells is low. Over 90% of the wells have been shut-in due to high water cut and low production rates. Since the proportion of inactive wells in the deepest reservoir intervals, J-IX to J-XIII, is higher than 65% (Table 2), there are many recompletion candidate wells for shallower intervals that may increase their utilisation rates. A large complex of sand bodies interpreted in logging data in the eastern part of horizon J-III (Figure 8), along with bright seismic amplitudes and the modelled remaining oil potential. From the results shown in this figure, we recommend increasing the reservoir throughput rate of J-III and the utilisation rates of old wells.

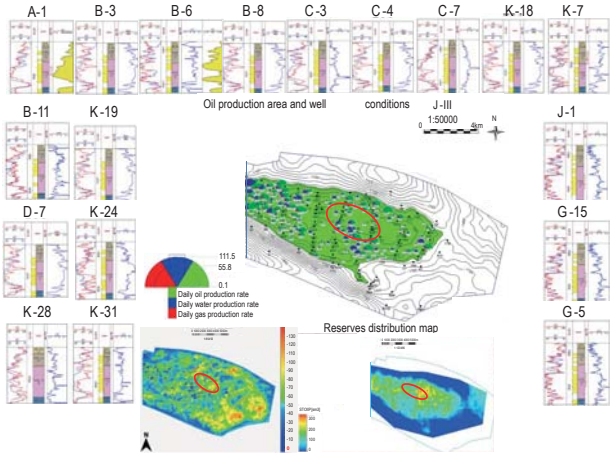

Figure 8. Map of the distribution of idle wells in the study area with remaining oil potential.

Table 2. Conditions of wells by reservoir interval.

Target horizon	Well stock of producing wells	Historical well stock of producing wells	Well stock of shut wells	Well stock of injection wells	Historical well stock of injection wells	Ratio of historical producing and shut wells (%)
J-II	0	2	2	0	0	100
J-III	18	100	31	42	32	30.69
J-IV	25	40	18	5	6	44.44
J-V	13	200	123	20	95	61.49
J-VI	10	150	91	18	89	60.77
J-VII	20	30	12	2	4	39.39
J-VIII	15	330	213	35	123	64.68
J-IX	44	120	93	15	28	77.32
J-X	13	400	291	48	143	72.83
J-XI	36	50	34	10	14	67.27
J-XII	6	350	295	24	101	84.21
J-XIII	5	80	76	1	1	95.33
Total	211	993	506	203	404	50.99

Dynamic analysis

Analyses of the water cut conditions of production wells within one reservoir interval and between neighbouring wells revealed the water cut amount of these wells varied widely. We took one group of wells in the southern part of horizon J-III as an example (Figure 9) to analyse the operating conditions of each well and found that wells Y-3, Y-7, Z-2, Z-4, and V had low water cuts and high oil production rates, while neighbouring wells had high water cuts. From the results of seismic

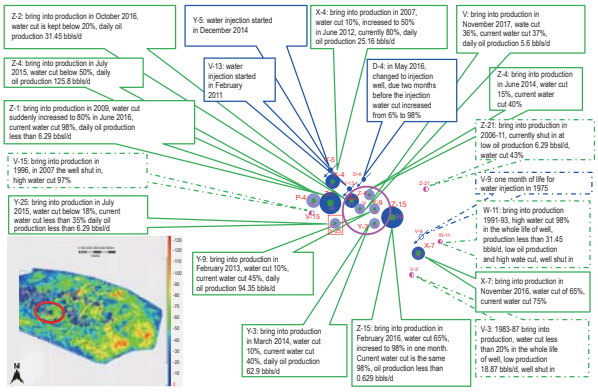

Figure 9. Dynamic analysis of well groups.

inversion, highly watered wells, such as Y-5, X-4, and X-7, were primarily found in the areas of sand body enrichment. In cross-sectional seismic inversions (Zabihi, 2016), low-water-cut wells, Z-4, Y-7, V, and Y-3, were located on the edge of the sand body and in the discontinuous area, and the remaining oil was relatively highly concentrated. Therefore, this is the main target area for drilling new wells and developing residual oil (Figure 10).

The first and most critical step for the joint impedance

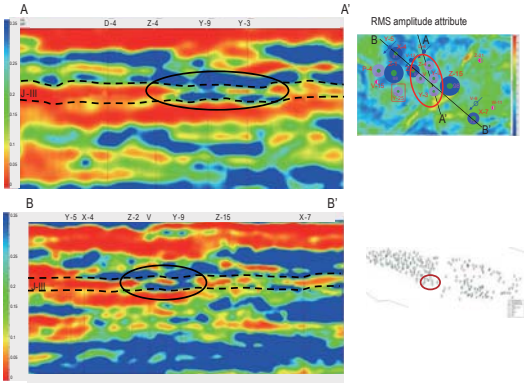

Figure 10. Cross-sectional seismic inversion of sandy clay rocks.

and facies-based inversion technique was to derive impedance depth trends for each facies. From these per-facies depth trends equivalent low frequency models are generated, an essential input to the algorithm. The depth trends, where the main facies are classified. The presence of soft shale can also be observed just above the reservoir. Separating the various shales into different facies types was a critical factor to improve the inversion accuracy. Facies based seismic inversion, a great tool to provide significant advantages over more conventional impedance inversion techniques. When facies-based inversion is combined with broadband data and appropriate broadband well tie techniques the resulting classified facies output provides a result ideally suited for geological interpretation and the generation of static and dynamic reservoir models. The inversion technique

successfully provides a better facies correlation with calibration wells. Also Inverts for an optimum low frequency model – thereby removing one of the most significant sources of error in more conventional simultaneous inversion techniques, where a low frequency model is an input, not an output. Therefore, it reduces interpretation burden by producing facies output akin to a geo-cellular model. Allows a full range of potential sensitivities to be explored therefore exploring the implications of inversion error.

Integrated analysis of geology, seismic attributes, and production performance

There is a wide distribution in the current water cut of the horizon J-III production wells, as well as a large proportion of high-water-cut wells. It can be seen that the water cut is the highest in the high-productivity wells of the main channel bodies, while lower productivity wells along the edge and lateral sides of the channel have lower degrees of flooding and thus higher potentials for remaining oil. Moreover, the cumulative production by well in horizon J-III is relatively high in the west and low in the east (Figure 11). Production wells on the lateral side of the channel also have low cumulative productions and low water cut levels. Consequently, in the eastern part and the lateral side of the channel, J-III has the highest potential for remaining oil, including a part with a low degree of involvement. Considering these results, horizon J-III is the key layer for tapping potential phase zones, as it has the following favourable conditions: relatively low oil recovery, substantial lateral variability in the reservoir, and regionally low water production.

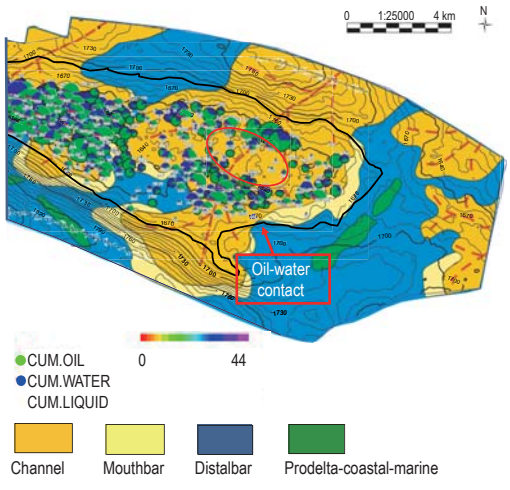

Figure 11. Overlay map of the accumulated production, sedimentary microfacies, and structure of horizon J-III.

Selection of potential sites

Based on previous studies, a geological model (Ibragimov et al., 2019) was constructed to estimate the volumes and distributions of remaining oil per reservoir interval (Figure 12). The distributions of initial oil shown in the maps suggest that the main production potential of horizon J-III is concentrated in the west and south, and this was confirmed by the cumulative well production (Figure 13). The area of poor deposit development, concentrated in the east, is the future target area for recompleting deeper wells and drilling new wells.

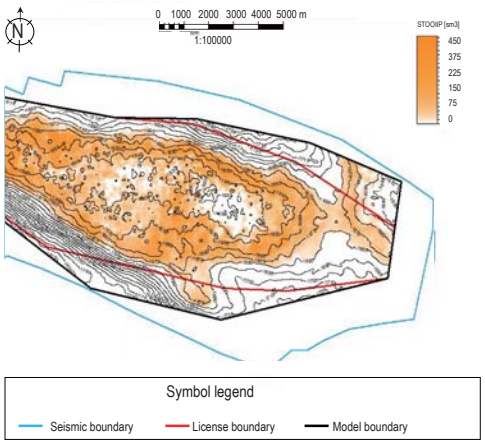

Figure 12. Distribution of oil resources in horizon J-III.

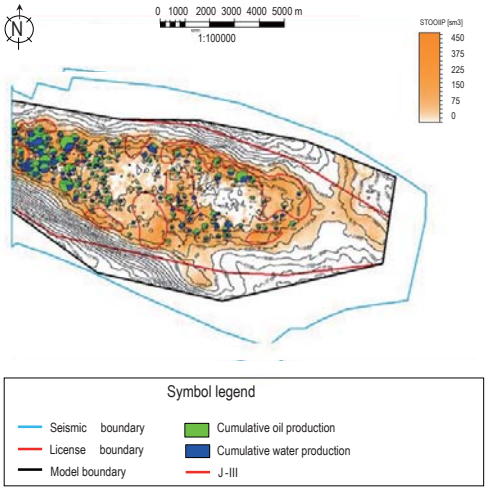

Figure 13. Overlay map of cumulative production, structure, and oil resources in horizon J-III.

A map of the locations and superpositions of favourable zones, with the distributions of drilled wells over the study area, was constructed according to the superposition of all of the identified potential sections

in the reservoirs. Potential sections of high interest were divided into two major regions — the areas of the recompleted wells and of the new wells. Currently, there is a large proportion of idle and shut-in deeper wells, but their potentials for recompletion are mainly concentrated in the central part of the oil reservoir. The area of new wells is therefore primarily located along the edges of the oil reservoir, where there is interpreted to be a high remaining oil potential. The potential redevelopment area was calculated to be 17.69 km2 for all layers and the proven undeveloped reserves for the J-III horizon were calculated to be ~29.5 MMbbl.

Results and new well development scenario

The first step that we recommend for recovering the remaining oil in the South Mangyshlak Sub-basin is to fully use the old well stock to recomplete wells for production from overlying horizons, which will provide quick and cost-effective potential sites. Our analysis of all shut-in and idle wells led to the selection of many wells suitable for recompletion from overlying horizons. As a result of analysing well dynamics, and in combination with potential sections, wells on horizon J-III were selected to recomplete from overlying horizons. According to the final proposal for horizon J-III, three wells are suitable for recompletion from overlying horizons and eight new wells are suitable for drilling in the southern part of the sub-basin (Figure 14).

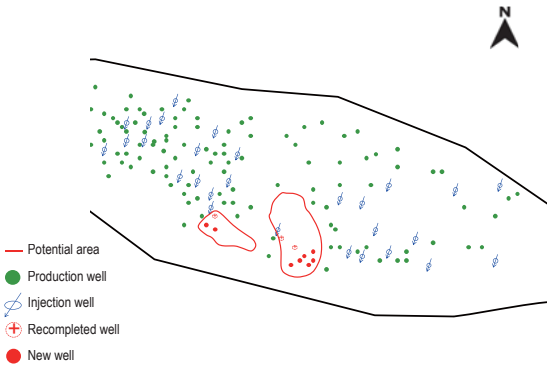

Figure 14. Map of the distribution of potential areas and proposed new well locations.

Using the map of the distribution of the proven undeveloped reserves (Figure 15), new wells were proposed for each reservoir interval. Then, shut-in deeper wells were recommended for secondary utilisation to produce from the overlying horizons. This approach of generating a development plan is iterative and was based on the map of undeveloped reserves. To increase the chance for the future redevelopment of closely spaced wells, we recommend drilling as many horizons as possible during the development of new wells.

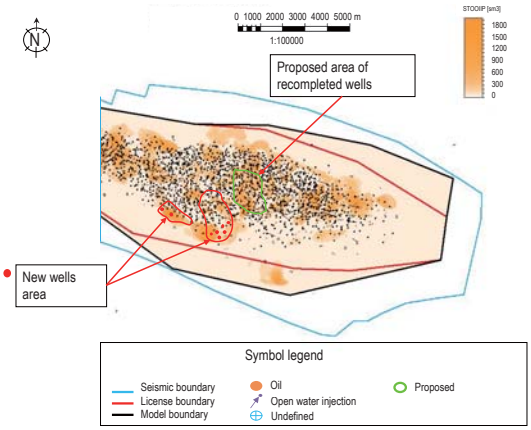

Figure 15. Map of the locations of new wells superimposed by the new undeveloped resources in horizon J-III.

Conclusions

Seismic data were used to constrain a structural and geological model of the study area, which provided the basis for adjusting the developmental approach of the oil reservoir and for assessing the exploration potential of the area. A comprehensive study using seismic inversion attributes and sedimentary microfacies revealed that reservoirs in the South Mangyshlak Sub-basin are mainly composed of deltaic deposits. Deposition in the reservoir included deltaic and branched channel sand bodies; the thickness of the sandstones varies markedly in the study area, and the lateral connectivity of the reservoir is complex. The main target horizon, J-III, contains four 4-branched deltas and channel sand bodies that are spread in a wide, perpendicular strip, with the distribution and productivity of hydrocarbons being determined by the facies characteristics. There is potential for redevelopment of the field; specifically, the low-seismic-amplitude traps at the edges of the study area appear to have potential. The geological models JI-J-XIII were collected, based on new seismic data and data on new wells, the geological model was updated, while the main data includes baseline log data for new

wells, structural surfaces of the packs in the depth area, data on the layering of formations at points-wells and conclusions on the interpretation of log data for new wells, which provided an update of the 3D geological model. Resources in the southern and central part of the area showed a great amount. Therefore, it is necessary to drill new wells to rapidly develop these field reserves.

The new, integrated workflow proposed here should enable the operating company to efficiently review production enhancement opportunities within the bypassed zones of reservoir layers, whether targeting structural or stratigraphic oil zones. Moreover, new drilling and workover opportunities to adjust new well locations, and access remaining oil have been generated at the edge of the main sand bodies and discontinuous areas identified from the seismic attribute. We ranked these targets based on their expected flow rates, ultimate recoveries, and associated reservoir and operational risks. This approach also provides a means of developing an in-depth understanding and for conducting a detailed exploration of the known best-producing areas that have historically been successfully drilled within the field.

Acknowledgements

We thank BGP Inc., China National Petroleum Corporation for their data support and assistance during the project. We would also like to thank the geophysical adviser and editor-in-chief at First Break, European Association of Geoscientists and Engineers, Peter Rowbotham, for additional scientific review and language assistance.

References

Aliyeva, E.H., 2009, Middle Caspian mesozoic petroleum system –terrigenous source-rocks and carbonate reservoirs: conference proceedings: SPE Europec featured 71st EAGE conference and exhibition, P172.

Arslan, I., Rajabi, F., and Ibrahima F., 2019, Practical automated detection of remaining oil in mature fields using production and geology data: SPE Western Regional Meeting, San Jose, California, USA, SPE-195321-MS, 1–21.

Avseth, P., Mukerji, T., and Mavko, G., 2010, Quantitative seismic interpretation: Cambridge University Press, Cambridge.

Berkhout, A.J., 1993, Seismic reservoir characterization: conference proceedings, 3rd EAGE International Congress of the Brazilian Geophysical Society, 1522–1525.

Brown, A.R., 1996, Seismic attributes and their classification: The Leading Edge, **15**(10), 1090–1090.

Cao, L., Xu, Y., and Yu, J., 2005, Facies analysis with merged 3D seismic data: 75th Ann. Internat. Mtg, Soc. Expl. Geophys., Expanded Abstracts, 613–616.

Carter, D.C., 2003, 3-D seismic geomorphology: insights into fluvial reservoir deposition and performance. Widuri field, Java Sea: AAPG Bulletin, **87**, 909–934.

Chen, X., Zhang, X., 2010, Study on four-property relationship of 6 reservoir in Nanniwan Oilfield. Journal of Sci-Tech Information Development and Economy, **20**, 163–166.

Chopra, S., and Marfurt, K.J., 2005, Seismic attributes — a historical perspective: Geophysics, **70**, 3–28.

Chopra, S., and Marfurt, K.J., 2014, Churning seismic attributes with principal component analysis: 84th Ann. Internat. Mtg, Soc. Expl. Geophys., Expanded Abstracts, 2672–2676.

Effimov, I., Downey, M.W., Threet, J.C., and Morgans, W.A., 2001, Future hydrocarbon potential of Kazakhstan, Petroleum Provinces of the 21st Century: AAPG Memoir, **74**, 243–258.

El-Mowafy, H.Z., and Marfurt, K.J., 2016, Quantitative seismic geomorphology of the middle frio fluvial systems, South Texas, United States: AAPG Bulletin, **100**, 537–564.

Gunter, G.W., Finneran, J.M., Hartmann, D.J., and Miller, J.D., 1997, Early determination of reservoir flow units using an integrated petrophysical method: SPE Annual Technical Conference and Exhibition, San Antonio, Texas, SPE-38679-MS, 1–8.

Harilal., Biswal, S.K., Sood, A., and Rangachari, V., 2008, Identification of reservoir facies within a carbonate and mixed carbonate-siliciclastic sequence: application of seismic stratigraphy, seismic attributes, and 3D visualization: the Leading Edge, **27**(1), 18–29.

Ibragimov, R., Ovchinnikov, A., Burdakov, D., Romantsov, A., Sterlyagova, S., Darmaev, B., and Zimin, S., 2019, Geology driven history match of eastern siberian halite cemented fluvial reservoir: SPE Abu Dhabi International Petroleum Exhibition & Conference, Abu Dhabi, UAE, SPE-197438-MS, 1–20.

Jing, W., Donghong, Z., Dingyou, L., Chengmin, N., Dianbo, H., Guoying, L., and Xiaoyuan, W., 2014, Structural interpretation of inner buried hill under restricted data availability - a case study in KL-X area,

Bohai Bay Basin: 84th Ann. Internat. Mtg, Soc. Expl. Geophys., Expanded Abstracts, 1689–1693.

Kazhegeldin, A.M., 1997, Oil and Gas Fields of Kazakhstan: Ministry of Ecology and Natural Resources, Almaty Press, **318**.

Kiritchkova, A.I., Timoshina, N.A., and Menshikova, N.Y., 1983, Stratigraphy of the Jurassic Deposits of Mangyshlak: Soviet Geology, **11**, 73–82.

Lechner, M., Iltukov, R., and Mukushev, M. A., 2016, Multidisciplinary approach to improve reservoir management of a tidal-fluvial channel reservoir in Tasbulat field, Kazakhstan: Conference Proceedings, SPE Europec featured at 78th EAGE Conference and Exhibition.

Li, J., Liu, Z., Lu, C., Li A., 2011, Study on the relationship of four characteristics in Dongzhuang reservoir. Journal of Oil-Gas Field Surface Engineering, **30**, 24–25.

Muruthy, S.P., and Ghosh, D.P., 2018, Integration of seismic attributes, petrophysics, and rock physics for depositional environment and facies characterization: Conference Proceedings, 1st EAGE-HAGI Asia Pacific Meeting, 1–5.

Pennington, W., 1997, Seismic Petrophysics: An applied science for reservoir geophysics: Geophysics, 16.

Posamentier, H.W., 2000, Seismic stratigraphy into the next millennium: a focus on 3D seismic data: AAPG Annual Convention Program, A118.

Smale, J.L., Dropkin, M., Bhattacharyya, D., Korsotyshevsky, M., Pronin, A., and Gaisina, S., 1997, Middle to upper Jurassic clastic reservoirs in the petroleum basins of Western Kazakhstan: parasequence architecture controls on hydrocarbon production: AAPG Bulletin, **81**, 1412–1413.

Soloviev, V., Gelman, V., Paduchih, V., Cherenov, V., and Solntsev, B., 2017, Geological structure and oil and gas potential of the platform part of the Caspian Sea: Neftegaz.ru, 1-8. https://neftegaz.ru/science/development/331536-geologicheskoe-stroenie-i-neftegazonosnost-platformennoy-chasti-kaspiyskogo-morya/ (In Russian).

Tang, M., Zhang, K., Huang, J., and Lu, S., 2019, Facies and the architecture of estuarine tidal bar in the lower Cretaceous McMurray formation, Central Athabasca Oil Sands, Alberta, Canada: Energies, **12**(1769), 1–18.

Ulmishek, G.F., 1990, Uzen Field - U.S.S.R., middle Caspian Basin, South Mangyshlak region: structural traps iv: tectonic and nontectonic fold traps: AAPG Special Volumes, 281–297.

Ulmishek, G.F., 2001, Petroleum geology and resources of the middle Caspian Basin, former Soviet Union: US Geological Survey Bulletin, 2201-a.

Walls, J., Dvorkin, J., and Carr, M., 2004, Well logs and rock physics in seismic reservoir characterization: SPE Offshore Technology Conference, Houston, Texas, OTC-16921-MS, 1–7.

Zabihi, N.E., 2016, Quantitative interpretation using facies based seismic inversion: SEG International Exposition and 86th Ann. Internat. Mtg, Soc. Expl. Geophys., Expanded Abstracts, 2906–2910.

Zhang, Y., Wang, H., Hu, X., Zhang, X., Pu, F., Gao, Y., and Fan, E., 2016, Reservoir modelling of complex lithologies with sparse wells: a case from a oilfield in Shijiutuo Uplift, Bohai Bay Basin: Oil Gas Geology (in Chinese, English abstract), **7**(3), 450–456.

Zudakina, Y.A., Yefremova, L.N., Vorontsova, G.I., and Rmyantsev, A.A., 1980 (English translation, 1981), Effect of conditions of sedimentation and of post-sedimentary alterations on reservoir properties of polymict sandstones of the Uzen Field: Petroleum Geology, **17**(7), 286–290.

Arslan Zhumabekov: He obtained a PhD in major geology and geological engineering from State Key Laboratory of Petroleum Resource and Prospecting in China University of Petroleum (Beijing) and Karaganda State Technical University. He has six-year experience in Geology, his research interests include geophysics and petroleum engineering, conceptualisation, and methodology.
E-mail address: zhak28@gmail.com (A. Zhumabekov).

Zhen Liu: Dr., Professor, State Key Laboratory of Petroleum Resource and Prospecting in China University of Petroleum. Research area is Geology, Geophysics and Petroleum Engineering.

Vasily Portnov: Second Co-Author: Professor, Dr, Supervisor-external adviser, Director, Head of the Geology and Geophysics Department, Karaganda State Technical University, Karaganda, 100027, Kazakhstan. Research area, 40-year experience in Geology, Geophysics Engineering and Geoscience. Supervision.